**Atmospheric
Chemistry
and Physics**

Ozone variability and halogen oxidation within the Arctic and sub-Arctic springtime boundary layer

J. B. Gilman[1,2], **J. F. Burkhart**[3], **B. M. Lerner**[1,2], **E. J. Williams**[1,2], **W. C. Kuster**[1], **P. D. Goldan**[1,2], **P. C. Murphy**[1,2], **C. Warneke**[1,2], **C. Fowler**[4], **S. A. Montzka**[1], **B. R. Miller**[1,2], **L. Miller**[1,2], **S. J. Oltmans**[1], **T. B. Ryerson**[1], **O. R. Cooper**[1,2], **A. Stohl**[3], and **J. A. de Gouw**[1,2]

[1]Earth System Research Laboratory (ESRL), NOAA, Boulder, CO, USA
[2]Cooperative Institute for Research in the Environmental Sciences (CIRES), University of Colorado, Boulder, CO, USA
[3]Norwegian Institute for Air Research (NILU), Kjeller, Norway
[4]Colorado Center for Astrodynamics Research (CCAR), University of Colorado, Boulder, CO, USA

Abstract. The influence of halogen oxidation on the variabilities of ozone (O_3) and volatile organic compounds (VOCs) within the Arctic and sub-Arctic atmospheric boundary layer was investigated using field measurements from multiple campaigns conducted in March and April 2008 as part of the POLARCAT project. For the ship-based measurements, a high degree of correlation ($r = 0.98$ for 544 data points collected north of $68°$ N) was observed between the acetylene to benzene ratio, used as a marker for chlorine and bromine oxidation, and O_3 signifying the vast influence of halogen oxidation throughout the ice-free regions of the North Atlantic. Concurrent airborne and ground-based measurements in the Alaskan Arctic substantiated this correlation and were used to demonstrate that halogen oxidation influenced O_3 variability throughout the Arctic boundary layer during these springtime studies. Measurements aboard the R/V *Knorr* in the North Atlantic and Arctic Oceans provided a unique view of the transport of O_3-poor air masses from the Arctic Basin to latitudes as far south as $52°$ N. FLEXPART, a Lagrangian transport model, was used to quantitatively determine the exposure of air masses encountered by the ship to first-year ice (FYI), multi-year ice (MYI), and total ICE (FYI+MYI). O_3 anti-correlated with the modeled total ICE tracer ($r = -0.86$) indicating that up to 73% of the O_3 variability measured in the Arctic marine boundary layer could be related to sea ice exposure.

1 Introduction

Long-term measurements of surface ozone (O_3) in the Arctic have shown that the greatest interannual variability occurs in the late winter and spring (Oltmans and Komhyr, 1986). During the Arctic springtime, surface O_3 can fluctuate between background levels of approximately 40 ppbv to near zero. While major ozone depletion events (ODEs, $O_3 < 4$ ppbv) are episodic in nature, they have been shown to occur perennially in the Arctic springtime boundary layer across the whole of the Arctic Basin (Oltmans and Komhyr, 1986; Bottenheim et al., 1990; Sturges et al., 1993; Solberg et al., 1996; Hopper et al., 1998; Ridley et al., 2003; Bottenheim et al., 2009; Hirdman et al., 2010). Air masses depleted in O_3 can remain so for several days due to the relatively stable and stratified nature of the Arctic boundary layer (Barrie and Platt, 1997; Stohl, 2006), which limits mixing with surrounding air masses. The most efficient way for an Arctic air mass depleted in O_3 to replenish itself is by mixing with O_3-rich air since photochemical O_3 production is generally not sufficient (Simpson et al., 2007b).

Observed O_3 depletions in the Arctic springtime boundary layer have been associated with air masses that were exposed to significantly enhanced concentrations of halogen atoms including atomic bromine (Br) and chlorine (Cl) radicals (Barrie et al., 1988; Oltmans et al., 1989; Jobson et al., 1994). It has been posited that Br is responsible for the near complete destruction of surface O_3 on the timescale of about a day by a photochemical, catalytic, chain-reaction; however, the mechanism in which the reactive halogens are liberated from the Arctic Ocean where they exist as inert halide salts

Correspondence to: J. Gilman
(jessica.gilman@noaa.gov)

is not entirely clear (Barrie et al., 1988; McConnell et al., 1992; Simpson et al., 2007b). Even though chlorine is the most abundant halide in seawater, the abundance of reactive Br atoms has been shown to exceed that of Cl by factors of 10^2–10^3 during ODEs (Jobson et al., 1994; Cavender et al., 2008). While Cl may not contribute much to O_3 destruction, Cl rapidly oxidizes a wide range of volatile organic compounds (VOCs) including alkanes, alkenes, and acetylene. Jobson et al. (1994) showed that the coincidental loss of a series of *n*-alkanes during ODEs could be readily explained by Cl oxidation kinetics. Acetylene was the only hydrocarbon that showed more decay than could be explained by Cl chemistry alone. Br oxidation was invoked in order to fully account for the loss of acetylene in O_3 depleted air masses. These observations directly link surface O_3 destruction and the oxidation of VOCs to the reactive halogens Cl and Br.

Previous studies have utilized modeled air mass back trajectories in order to identify possible source regions of O_3 depletion chemistry. These studies showed that air masses depleted in O_3 had advected over the predominately ice- and snow-covered Arctic Ocean (Hopper et al., 1998) or over open leads in the sea ice (Sturges et al., 1993). Arctic sea ice can be divided into two main categories: multi-year ice (MYI) and first-year ice (FYI). MYI has survived the annual melt, which typically peaks in September in the Arctic, whereas FYI is formed subsequent to the annual melt. While FYI can eventually evolve into MYI, the two types of ice differ geographically, chemically, and physically. MYI is located primarily in the western Arctic near Greenland and the Canadian archipelago while FYI forms in the eastern (Siberian) Arctic and is transported westward across the pole (Fowler et al., 2004; Belchansky et al., 2005). FYI has been shown to have a higher salinity than MYI particularly during the initial freezing process, which forms a concentrated brine layer at the surface (Notz and Worster, 2008). Additionally, open leads and polynyas, semi-permanent areas of open water surrounded by sea ice, are often associated with areas of FYI because it is thinner and more susceptible to fragmentation by the wind and ocean currents. Open leads and polynyas can be a direct source of sea-salt aerosols or they can be covered by a thin layer of ice allowing for the growth of saline crystals called frost flowers (Martin et al., 1995; Kaleschke et al., 2004). While young sea ice has been implicated in halogen activation and O_3 depletion (Wagner et al., 2001; Simpson et al., 2007a; Bottenheim et al., 2009), MYI has not generally been considered to be a strong source of the reactants required for O_3 destruction chemistry.

A series of concurrent field observations from multiple platforms were conducted in spring 2008 as part of POLARCAT (Polar Study using Aircraft, Remote Sensing, Surface Measurements and Models, of Climate, Chemistry, Aerosols, and Transport, http://www.polarcat.no/), which was a large international program organized as part of the 2007–2008 International Polar Year. In this work, results from (1) ICEALOT (International Chemistry Experiment in the Arctic

Lower Troposphere), a ship-based study in the North Atlantic and Arctic Oceans aimed at characterizing the atmospheric composition of the ice- and snow-free regions of the Arctic, (2) ARCPAC (Aerosol, Radiation, and Cloud Processes affecting Arctic Climate), an airborne study over northern Alaska and the frozen Beaufort Sea, and (3) ground-based measurements at Barrow, Alaska, are used to investigate the influence of halogen oxidation on O_3 variability within the Arctic and sub-Arctic. Data from two mid-latitude studies on the Atlantic and Pacific coasts (2004 New England Air Quality Study and Trinidad Head, CA, respectively) are compared to the Arctic datasets in order to investigate the broader, spatial-scale variations in O_3. Lastly, FLEXPART, a Lagrangian particle dispersion model (Stohl et al., 2002, 2005), was used to quantitatively determine the exposure of air masses sampled during ICEALOT to FYI, MYI, and total ICE (FYI+MYI) in order to determine if the variability in O_3 could be explained by the exposure to specific types of sea ice.

2   Experimental

2.1   Ship-based measurements in North Atlantic and Arctic Oceans

The International Chemistry Experiment in the Arctic Lower Troposphere (ICEALOT) was conducted aboard the R/V *Knorr* in the North Atlantic and Arctic Oceans in March and April 2008 as part of the larger POLARCAT program. The cruise track of the R/V *Knorr*, operated by Woods Hole Oceanographic Institution, is shown in Fig. 1 and has been colored by measured O_3 mixing ratios. The cruise has been divided into four areas of study which include the northeastern United States (NE US, 41° N to 45° N), the sub-Arctic (45° N to 68° N excluding Iceland leg of cruise), the Arctic (68° N to 80° N), and Iceland (IS, 62° N to 68° N).

A full suite of volatile organic compounds (VOCs), including C2-C6 hydrocarbons, C2-C4 oxygenated VOCs, C6-C9 aromatics, halogenated VOCs, alkyl nitrates, dimethyl sulfide (DMS), and acetonitrile, were measured in situ by a custom built, two-channel, gas chromatograph-mass spectrometer (GC-MS). The inlet for the GC-MS consisted of a 30 m unheated Teflon line, which was positioned on the forward mast of the R/V *Knorr* approximately 25 m above the waterline. Ambient air was pulled continuously at a rate of approximately 7 L min^{-1} through the inlet line resulting in an inlet residence time of approximately 3 s. From this high-flow sample stream, two separate ambient air samples were collected simultaneously at a flow rate of 70 sccm for a total of 5 min via cryogenic trapping. The two sample channels have slightly different configurations designed to reduce water and carbon dioxide and remove O_3 from the sample stream prior to trapping as described in Goldan et al. (2004). After the 5 min sample acquisition period, the two samples

Table 1. Summary of the measurement parameters, statistics, and reaction rate coefficients for OH (k_{OH}), Cl (k_{Cl}), and Br (k_{Br}) with a select group of VOCs measured during ICEALOT. The mean, median, maximum, and minimum values are for the 891 VOC samples in the sub-Arctic and Arctic.

Compound	LOD	Precision	Accuracy	Mean	Median	Max	Min	kOH at 250 K	kCl at 250 K	kBr at 250 K
	ppb			*ppb*	*ppb*	*ppb*	*ppb*	10^{12} cm^3 s^{-1}	10^{12} cm^3 s^{-1}	10^{12} cm^3 s^{-1}
Ethane	0.0100	8%	15%	1.694	1.731	2.145	0.976	0.12 [A]	55.6 [A]	NR
Propane	0.0100	6%	15%	0.654	0.682	*1.289*	**0.176**	0.72 [A]	141 [A]	NR
i-Butane	0.0050	5%	15%	0.106	0.100	*0.309*	**0.028**	1.71 [B]	137 [F*]	NR
n-Butane	0.0050	5%	15%	0.182	0.190	*0.941*	**0.027**	1.78 [B]	198 [F*]	NR
i-Pentane	0.0010	5%	20%	0.056	0.058	*0.392*	**0.008**	3.60 [B*]	203 [F*]	NR
n-Pentane	0.0010	5%	20%	0.051	0.051	*0.441*	**0.006**	2.96 [B]	311 [G*]	NR
n-Hexane	0.0010	5%	20%	0.011	0.012	*0.116*	**0.001**	5.2 [B*]	345 [G*]	NR
Acetylene	0.0100	10%	20%	0.365	0.376	0.562	**0.071**	0.78 [C*]	71 [G*]	0.154 [K*]
Benzene	0.0005	3%	20%	0.097	0.099	0.127	0.054	0.91 [C]	4.0 [G*]	NR
Acetaldehyde	0.0010	15%	25%	0.065	0.056	0.334	**0.004**	19.1 [A]	72 [A]	3.08 [L]
Propanal	0.0010	15%	25%	0.029	0.023	0.189	**0.005**	25.8 [A]	120 [A*]	9.73 [L*]
Butanal	0.0010	15%	25%	0.013	0.009	0.130	**0.002**	30.9 [A]	137 [H*]	20 [M]
Acetone	0.0100	15%	25%	0.476	0.473	0.962	0.158	0.14 [D]	1.42 [I]	NR
2-Butanone	0.0100	15%	25%	0.070	0.068	0.317	0.025	1.17 [A]	37.5 [I]	NR
Bromoform	0.0005	10%	20%	0.002	0.002	**0.004**	0.001	0.12 [E]	0.22 [J*]	NR

LOD = Limit of detection; Precision = Reproducibility; *Italic* = Associated with Kola Peninsula plume sampled on 8 April 2008; **Bold** = Associated with ozone depletion event sampled 15–20 April 2008; [A] = Atkinson et al. (2001); [B] = Atkinson et al. (2003); [C] = Atkinson (1986); [D] = Wallington and Kurylo (1987); [E] = DeMore et al. (1997); [F] = Atkinson and Aschmann (1985); [G] = Wallington et al. (1988); [H] = Cuevas et al. (2006); [I] = Zhao et al. (2008); [J] = Kamboures et al. (2002); [K] = Barnes et al. (1993); [L] = Wallington et al. (1989); [M] = Ramancher et al. (2000) NR = Negligible Reactivity; * denotes rate coefficients at 298 K

are transferred to cryofocus units positioned at the heads of the two GC columns. Channel one (CH1) consists of an 18 m Al_2O_3/KCl PLOT column, and the second channel (CH2) utilizes a semi-polar 20 m DB-624 capillary column. After the sample transfer is complete, the cryofocus unit on CH1 is then flash heated from $-165\,°C$ to $100\,°C$ in 0.2 s injecting the sample onto the CH1 column for subsequent analysis by a linear quadrupole mass spectrometer (Agilent 5973). While the CH1 sample is being analyzed, the CH2 sample is held in its cryofocus unit for an additional 192 seconds. When the analysis of the CH1 sample is near completion, the cryofocus unit on CH2 is flash heated injecting the sample onto the CH2 column. Immediately after injection, a 4-way pneumatic valve (Valco Instruments Co. Inc., Houston, TX) located upstream of the mass spectrometer switches so that the sample eluting from the CH2 column is now directed to the detector while the remaining CH1 carrier gas is vented. The entire sample collection (5 min) and analysis sequence (25 min) repeats automatically every 30 min beginning on the hour and half-hour. The detection limits and uncertainties of the VOC measurements detailed this study are compiled in Table 1. The gas-phase data have been filtered for contamination by the ship itself.

O_3 was measured via UV absorbance by a commercial instrument (Thermo Environmental Instruments, Inc., Model 49c). Carbon monoxide (CO) was measured by a vacuum-UV resonance fluorescence instrument (Gerbig et al., 1999). The O_3 and CO measurements presented in this analysis rep-resent 5 minute averages coincident with the GC-MS sample acquisition. Radon measurements, detailed in Bates et al. (2008), are 30 min averages which overlap with each of the GC-MS samples.

2.2 Airborne measurements in Alaskan Arctic

The Aerosol, Radiation, and Cloud Processes affecting Arctic Climate (ARCPAC) study, which was part of the larger POLARCAT program, was conducted in Fairbanks, Alaska, in April 2008 using the NOAA WP-3D aircraft. NOAA whole air samples (NWAS) were collected in glass flasks during the research flights that were made over northern Alaska and the frozen Beaufort Sea. The flasks were transported to the NOAA Global Monitoring Division laboratory in Boulder, Colorado, where they were analyzed within a few days for hydrocarbons and halocarbons using GC-MS (Montzka et al., 1993; Warneke et al., 2009). The limit of detection for the VOCs in the NWAS is approximately 5 ppt. The NWAS acetylene results have been multiplied by a factor of 1.3 so that the acetylene measurements were on a consistent scale with the shipboard in situ GC-MS. The factor of 1.3 is based on measured differences in the calibration standards of acetylene used by the different research groups. We have not attempted to resolve here which standards are more accurate.

During ARCPAC, O_3 was measured with a 50 pptv limit of detection and 4% uncertainty on a 1-s time base using NO-induced chemiluminescence (Ryerson et al., 1998). O_3
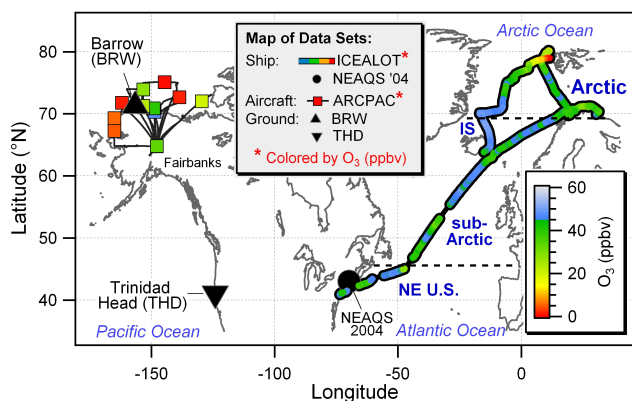
Fig. 1. Locations of the data sets used in this analysis. The four data subsets of the ICEALOT campaign aboard the R/V *Knorr*, which include the northeastern United States (NE US), sub-Arctic, Arctic, and Iceland (IS), are identified. The ICEALOT ship track and the flask samples collected along the ARCPAC flight tracks in Northern Alaska are colored by measured O_3 mixing ratios. Additional data sets include flask samples collected at ground-based observatories in Barrow, Alaska, (BRW) and Trinidad Head, California, (THD) as well as ship-based studies from the 2004 New England Air Quality Study (NEAQS '04) aboard the R/V *Brown*.

mixing ratios were averaged over the NWAS collection time, which ranged from 6 to 15 s depending on altitude. In the analysis presented here, only the measurements of acetylene and benzene in the 14 NWAS that were collected below 1 km in altitude and had mean CO mixing ratios of less than 190 ppbv are included. Samples with mean CO > 190 ppbv have been excluded from this analysis as these samples are considered to be significantly above the Arctic springtime background of 160 ppbv (Warneke et al., 2009) due to contributions from biomass burning. Figure 1 shows the flight tracks and sampling locations of each of the NWAS, which have been colored by their respective mean O_3 mixing ratios.

2.3 Ground-based measurements in Barrow, AK and Trinidad Head, CA

The Barrow, Alaska, Observatory (BRW at 71.32° N, 156.61° W) is located approximately 8 m above sea level near the northernmost point of the United States. The prevailing winds at BRW are from the east-northeast off the Beaufort Sea (Oltmans and Levy, 1994). The Observatory at Trinidad Head, California, (THD at 41.05° N, 124.15° W) is located on the northern coast of California about 100 m above sea level. THD is a relatively remote, mid-latitude, coastal site with prevailing maritime airflow off the Pacific Ocean (Oltmans et al., 2008). NOAA whole air samples are collected in stainless steel canisters at both surface sites on a weekly basis year round, but only a subset of those flasks are analyzed for acetylene on the same instrument and by the same procedures as described in Sect. 2.2.

O_3 is measured by UV absorption at both surface sites year round (Oltmans and Levy, 1994). The O_3 measurements presented here are hourly averages encompassing the time that each flask was filled. The data collected at the surface sites during January through May of 2008 and January to February of 2009 are included in this analysis. This dataset represents the entire acetylene record at both sites for winter and spring that was available at the time of this analysis.

2.4 FLEXPART model description

FLEXPART, a Lagrangian particle dispersion model, has been extensively validated (Stohl et al., 1998, 2003) and has been used to investigate long-range transport to the Arctic (Stohl, 2006; Warneke et al., 2009, 2010; Hirdman et al., 2010). The FLEXPART model differs from traditional isentropic back trajectories in that thousands of particles are released and subjected to atmospheric dynamics including mean wind fields, convection, and turbulence (Stohl et al., 2002, 2003, 2005, see also http://transport.nilu.no/flexpart). For this analysis, each release consisted of 60 000 particles. Releases occurred every 30 min, or sooner if there was a shift in wind direction greater than 15° or if the ship moved more than 0.18° in latitude or longitude, for a total of 1,735 releases along the cruise track. The paths of the particles in each release were then tracked for 20 days back in time using the mean winds interpolated from the European Center for Medium-Range Weather Forecasts (ECMWF) operational analyses with 0.5° × 0.5° resolution. The wind fields were updated every three hours beginning at midnight UTC.

The backward simulations of the paths of the particles were mapped onto a uniform 3-dimensional grid as a function of time since the release. From the particle locations, FLEXPART provides a Potential Emission Sensitivity (PES) function, a so-called source-receptor-relationship (Seibert and Frank, 2004). The PES value (in units of s kg^{-1}) in a particular grid cell is proportional to the residence time of the particle in that grid cell (Hirdman et al., 2010). This analysis utilizes the PES value for the footprint layer, which is defined in the model as the lowest 100 m of the atmosphere. All particles that reside within this shallow layer are presumed to be in contact with Earth's surface. While the generally stratified nature of the Arctic boundary layer can lead to gradients within this 100 m layer, field measurements in the Arctic aboard the R/V *Knorr* (Lerner et al., 2010) and NOAA WP-3D (Neuman et al., 2010) indicate that the atmospheric boundary layer depth was no less than 150 m when air masses with depleted O_3 were observed.

The PES values (s kg^{-1}) for the footprint layer were then folded with gridded "sea ice emission fluxes" (units of kg s^{-1} m^{-2}). In this application of FLEXPART, the modeled emission is of an inert "FYI or MYI tracer." This is analogous to the FLEXPART modeling of an atmospheric tracer such as CO at a receptor site based on emission fluxes of CO from a gridded emission inventory (Stohl et al., 2003).

First-year ice (FYI) or multi-year ice (MYI) within a particular grid cell is assigned an arbitrary unit emission of $1.0\,kg\,s^{-1}\,m^{-2}$, while grids comprised of open water or land were assigned an emission of $0.0\,kg\,s^{-1}\,m^{-2}$. The FYI or MYI tracers are assumed to be instantaneously mixed within the gridded footprint volume upon emission. The sea ice was classified as FYI or MYI by the procedures outlined in Fowler et al. (2004). The sea ice coverage maps and classifications were updated weekly. The result of folding the footprint PES values with the gridded FYI or MYI emission fluxes is a map of the sea ice source contribution (units of $ppbv\,m^{-2}$), which depicts the magnitude and location of the particles' exposure to FYI or MYI tracer emissions.

By summing up all the FYI or MYI Source Contributions from each grid cell and integrating over the grid area (units of m^2), the mixing ratio of the inert FYI or MYI tracers (in units of ppbv) can be determined for each release along the ship track for 1 to 20 days prior to the initial release. While the amount of the FYI and MYI tracers are quantitative, the absolute scale is arbitrary due to the fact that a unit emission factor of a fictitious tracer was used. The term "exposure" used throughout this text is defined here as the modeled quantity (ppbv) of the specified type of inert ice tracer, which is directly proportional to the time that an air mass was in contact with the specified types of sea ice. Examples of the various FLEXPART model outputs are further discussed in Sect. 3.4.

3 Results and discussion

3.1 VOC ratios as oxidation markers

Primary oxidants of VOCs in the Arctic springtime include the hydroxyl radical (OH) and the halogen atoms Br and Cl (Jobson et al., 1994). These oxidants determine the chemical lifetimes of VOCs that are emitted or transported into the Arctic. The reactivities of VOCs with OH, Cl, and Br can be used to determine the relative importance of the different oxidants (Jobson et al., 1994; Ramacher et al., 1999; Cavender et al., 2008). For example, the propane to i-butane ratio (denoted as [Propane]/[i-Butane]) is used throughout this analysis as a marker for OH oxidation. OH oxidation will cause [Propane]/[i-Butane] to increase because i-butane is oxidized by OH approximately 2.4 times faster than propane based on the reaction rate coefficients listed in Table 1. While [Propane]/[i-Butane] is sensitive to OH oxidation, it will not be affected by Cl oxidation as propane and i-butane have similar Cl reaction rate coefficients, which only differ by a factor of 1.03.

Cl oxidation is indicated by decreases in [n-Butane]/[i-Butane]. n-Butane reacts 1.4 times faster with Cl than i-butane. This ratio is not sensitive to OH oxidation as both isomers have similar OH reactivities within a factor of 1.04. Neither of the alkane ratios used as OH or Cl oxidation mark-

ers will be affected by Br. Br only reacts at appreciable rates with a select group of VOCs including ethene, acetylene, aldehydes, and some halocarbons. A decrease in [Acetylene]/[Benzene] is used throughout this study as an indicator of halogen oxidation as acetylene is more readily oxidized by both Br and Cl than benzene.

VOC ratios are generally less sensitive to dilution and mixing than the absolute concentrations of individual species (Parrish et al., 2007). We note that VOC ratios can be perturbed by 1) the mixing of air parcels that have been exposed to sources with disproportionate emission ratios of the specified hydrocarbons or 2) the mixing of air parcels that have been exposed to vastly different degrees of chemical processing. In the following discussions, we compare the variability in the VOC ratios to other trace gases in order to isolate the influence of halogen oxidation from any perturbations linked to the mixing of disparate air masses.

3.2 Description of ICEALOT data subsets

Figure 2a–e shows the time series for wind direction, temperature, O_3 and the VOC ratios used as oxidation markers. At the start of the cruise, the R/V *Knorr* sampled off the northeastern coast of the United States (NE US). Much of the air sampled within this region is characterized as urban outflow where O_3 was negatively correlated with CO and nitric oxide (NO, not shown) due to NO titration of O_3. The ship briefly sampled a distinctly different air mass on 25 March 2008. The arrival of this air mass was signaled by an abrupt change in the wind direction, sharp increases in the air temperature and absolute humidity (not shown), and decreases in O_3, CO, and certain VOCs. This air mass, determined to be sub-tropical in origin, was transported northward as a result of a mid-latitude cyclone positioned to the southwest of the ship. We do not further interpret the fine-scale variabilities of the VOC ratios in the NE US data subset, as the ratios were likely influenced by the mixing of urban or sub-tropical air masses with background air rather than by specific types of oxidation.

Within the sub-Arctic region, there were distinct decreases in O_3 that were not associated with changes in wind direction, temperature, or CO (Fig. 2). For example, O_3 decreased from 45 to 32 ppbv on 28 March 2008. During this time, there were simultaneous decreases in [Acetylene]/[Benzene] and [n-Butane]/[i-Butane] while [Propane]/[i-Butane] remained constant indicating that this air mass was predominately exposed to halogen oxidation. FLEXPART indicates that this air mass originated in the Arctic before advecting over northeastern Canada, Baffin Bay, and the Davis Strait. Shortly after this period, the general paths of the air masses shifted from the western (Canadian) Arctic to the eastern (Siberian) Arctic. On 6 April 2008 when the R/V *Knorr* was positioned along the northern coast of Norway, another concurrent and prolonged decrease in [Acetylene]/[Benzene] and O_3 was observed indicating the influence of halogen
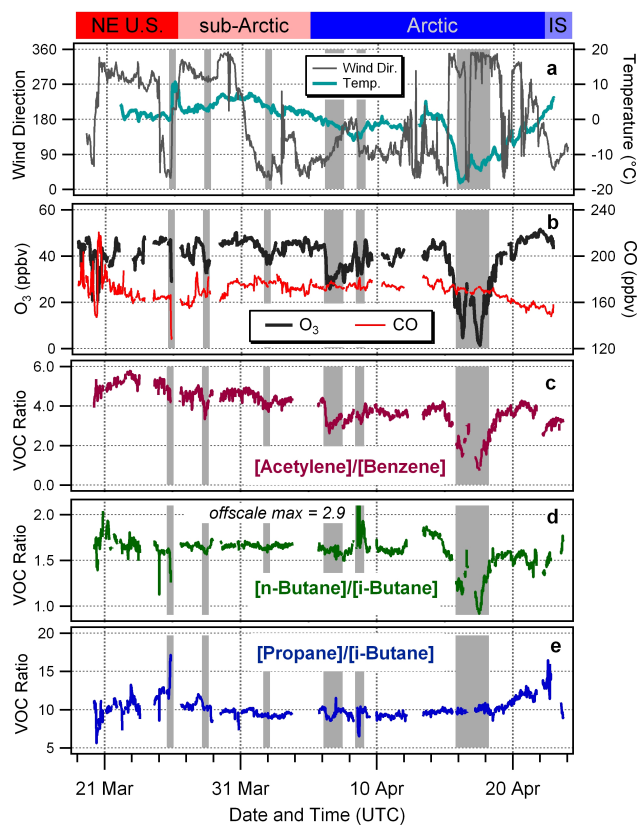
Fig. 2. Time series of **(a)** wind direction and ambient temperature, **(b)** O_3 and CO, **(c)** [Acetylene]/[Benzene] which is used as a marker for Cl and Br oxidation, **(d)** [n-butane]/[i-butane] which is used as a marker for Cl oxidation, **(e)** [Propane]/[i-butane] which is used as a marker for OH oxidation. The ICEALOT data subsets are delineated at the top. The grey bands highlight specific samples that are discussed in the text.

oxidation (Fig. 2); however, a small decrease in [Propane]/[i-Butane] points to the possible influence of the mixing of two air masses with different VOC emission source ratios or different degrees or types of chemical processing. FLEXPART determined that this air mass originated in the central/eastern Arctic, advected southward towards the Kola Peninsula, before shifting westward and advecting along the northern European coastline prior to interception by the ship.

A plume enriched in hydrocarbons was encountered on 8 April 2008 as the R/V *Knorr* traveled eastward towards the Norwegian/Russian border. The enrichment of the C3-C5 alkanes, determined by comparing the maximum values listed in italics in Table 1 to their median values, increased according to carbon number and was greater for the linear alkanes compared to their branched isomers. This resulted in the sharp increase in [n-Butane]/[i-Butane] and decrease in [Propane]/[i-butane] as shown in Fig. 2d and 2e, respectively. FLEXPART shows that this air mass had advected over the Kola Peninsula near the city of Murmansk, Rus-
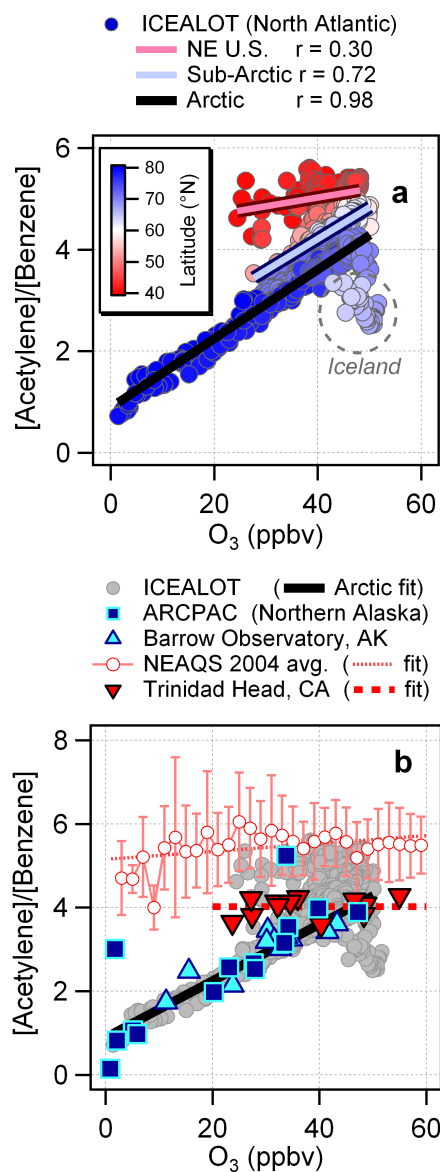
Fig. 3. (a) Scatter plots of [Acetylene]/[Benzene] versus O_3 for the ICEALOT campaign. The data points have been colored by latitude. Linear fits and corresponding correlation coefficients for the NE US, sub-Arctic, and Arctic data subsets of the ICEALOT campaign are included. **(b)** Scatter plots of [Acetylene]/[Benzene] versus O_3 for the flask samples from ARCPAC, Barrow, and Trinidad Head as well as the mean [Acetylene]/[Benzene]$\pm 1\sigma$ from NEAQS 2004. Linear fits to Trinidad Head and NEAQS 2004 datasets are shown. The ICEALOT data and fit to the Arctic data subset, which appear in panel (a), have been included in panel (b) for comparison.

sia, which represents a local, anthropogenic, point source of VOCs that is likely associated with natural gas processing, which is common to the area. This point source had a distinctive VOC source signature, which resulted in the perturbation of the alkane ratios used as oxidation markers. These perturbations are consistent with those observed on 6 April

2008 suggesting that a halogen oxidized air mass may have been mixed with air that was at least partially enriched in alkanes.

A prolonged period of reduced O_3 was observed from 15–19 April 2008 when the ship was near the coast of Svalbard, Norway, and in close proximity (0.5 to 2.0 km) to sea ice. During this time, the wind was predominately from the north-northwest. The ambient temperature reached a minimum of $-18\,^\circ$C, and O_3 was reduced from 43 ppbv to 1.5 ppbv as shown in Fig. 2a, b. FLEXPART indicates that the air masses sampled throughout this time period were entirely Arctic in origin, having been confined to latitudes north of 80° N for the majority of their 20-day histories. The strong association between the time series of O_3, [Acetylene]/[Benzene], and [n-Butane]/[i-Butane], as shown in Fig. 2b–e, indicates that this air mass had been exposed to both Cl and Br oxidation. The [Br]/[Cl] ratio can be derived from the relative change in a VOC's mixing ratio from its "background" value (i.e., outside of an ODE) to that observed in a halogen oxidized air mass (Jobson et al., 1994; Ramacher et al., 1999). Lerner, et al. (2010) presents this type of analysis for the large-scale ODE encountered during ICEALOT and determined a mean [Br]/[Cl] ratio of 1600±200. This ratio is consistent with previously reported [Br]/[Cl], which range from approximately 400 to 2000 (Jobson et al., 1994; Cavender et al., 2008).

The gradual increase in [Propane]/[i-Butane] from 20 April 2008 to the end of the cruise in Iceland (Fig. 2e) indicates the growing influence of OH chemistry in the Arctic and sub-Arctic in the late spring. During this time period, CO gradually decreased while O_3 reached a campaign maximum of 51 ppbv. The atmospheric lifetime of CO is largely controlled by reaction with OH, and OH radicals are responsible for the photochemical production of O_3. FLEXPART indicates that the air masses sampled during this time had large footprint emission sensitivities to Eastern Europe. The previously noted changes in CO, O_3, and the VOC ratios towards the end of the campaign are likely influenced by the mixing of background air in the Arctic with air from more southerly regions where OH oxidation is increasingly important.

3.3 Halogen oxidation and O_3 variability

A scatter plot of [Acetylene]/[Benzene] versus O_3 is used here to assess the impact of halogen oxidation on the variability of surface O_3. Figure 3a includes the ICEALOT data, which has been colored by latitude, as well as the linear regressions and corresponding correlation coefficients for the NE US ($r = 0.30$), sub-Arctic ($r = 0.72$), and Arctic ($r = 0.98$) data subsets. The correlation between [Acetylene]/[Benzene], which is sensitive to Br+Cl oxidation, and O_3 strengthened as the R/V *Knorr* sailed north towards the Arctic. The fit for the Arctic data subset shows a high degree of correlation with r = 0.98 for the 544 data points collected north of 68° N. When the analysis is expanded to include the additional 347 data points collected in the sub-Arctic, the correlation for the combined Arctic and sub-Arctic region remains strong with $r = 0.90$. The strength of the correlation between [Acetylene]/[Benzene] and O_3 in the Arctic and sub-Arctic is remarkable given that the sources and atmospheric fates of these species are often quite different; however, one factor linking O_3 and acetylene is their common sensitivity to halogen oxidation. The strong correlation between [Acetylene]/[Benzene] and O_3 indicates that halogen oxidation accounted for up to 96% ($r = 0.98$, $r^2 = 0.96$) of the variability in O_3 measured in the Arctic marine boundary layer in the springtime during ICEALOT.

We have established for the ICEALOT dataset that concurrent reductions in [Acetylene]/[Benzene] and O_3 can be accounted for by the oxidation of acetylene via Cl and Br and the destruction of surface O_3 by Br. These concurrent reductions result in the observed slope of the Arctic fit to the ICEALOT data set (Fig. 3a), which is determined by comparing Arctic "background" values (e.g., $O_3 = 45$ ppbv and [Acetylene]/[Benzene] = 4.0) to air masses that have been exposed to halogen oxidation (e.g., $O_3 = 1.5$ ppbv and [Acetylene]/[Benzene]= 1.0). It is interesting to note that the slope of the sub-Arctic fit (Fig. 3a) is similar to that of the Arctic; however, the y-intercept is greater for the sub-Arctic data subset. As shown in Fig. 2, [Acetylene]/[Benzene] decreases from a mean value of 5 in the NE U.S. to a mean background value of approximately 4 in the Arctic. The offset in the [Acetylene]/[Benzene] for the sub-Arctic data subset is reflective of the waning influence of continental outflow from North America and the increasing influence of Arctic outflow as the R/V *Knorr* sailed northward. The observed slope, y-intercept, and strength of the correlation between [Acetylene]/[Benzene] and O_3 for the sub-Arctic dataset indicates that halogen oxidation, which likely occurred in the Arctic high latitudes, influenced O_3 variability in the sub-Arctic.

Figure 3b compares the ICEALOT dataset to other measurements in the Arctic and at coastal mid-latitudes in order to gauge the spatial extent of halogen oxidation influence on surface O_3 variability. The data from two springtime studies in Alaska, ARCPAC and Barrow (BRW), exhibit similarly high degrees of correlation between [Acetylene]/[Benzene] and [O_3] with $r = 0.81$ ($r = 0.98$ without the two outliers) and $r = 0.89$, respectively, and the majority of the data from the Alaskan studies fall on the Arctic fit to the ICEALOT data collected on the opposite side of the Arctic. This implies that halogen oxidation can account for the vast majority of the observed O_3 variability throughout the Arctic boundary layer during these springtime studies. The fact that the Alaskan studies have a similar slope as the Arctic fit to the ICEALOT data suggests that halogen oxidation chemistry may be comparable across the Arctic (i.e., similar reactant ratios and reaction conditions) and/or the mixing/dilution of halogen oxidized air masses within the arctic boundary layer do not significantly perturb the relationship between

[Acetylene]/[Benzene] and O$_3$. While it is difficult to distinguish between these scenarios with the available datasets, Jobson et al. (1994) suggested that the effects of mixing and dilution of air masses on VOC ratios measured within the Arctic will be minimal because of the narrow range of air mass photochemical ages.

Measurements from two mid-latitude coastal sites have been added to Fig. 3b for comparison. The New England Air Quality Study (NEAQS) was conducted along the northeastern coast of the US aboard the NOAA R/V *Brown* in the summer of 2004 (Warneke et al., 2007). [Acetylene]/[Benzene] from NEAQS is comparable to that measured during the springtime ICEALOT cruise in a similar geographic region. However, [Acetylene]/[Benzene] and O$_3$ were not significantly correlated in the NE US data subset ($r = 0.30$) or during NEAQS ($r = 0.004$) indicating that halogen oxidation was not a large factor in determining O$_3$ variability in this region in either spring or summer. This is in accordance with the findings of Keene et al. (2007) who determined that Br chemistry is relatively unimportant in the evolution of polluted coastal air in this region.

The Observatory at Trinidad Head, California, (THD) is located along the Pacific coast at approximately the same latitude as the east coast studies (Fig. 1). Oltmans et al. (2008) determined that approximately 25% of the air masses reaching THD in April originate in northern Alaska and are transported at relatively low altitudes throughout their modeled 10-day trajectories. Figure 3b shows that [Acetylene]/[Benzene] is independent of O$_3$ at THD in late winter and spring. Even though a fraction of the air masses reaching THD in the spring may have originated in the Arctic, there is no indication that O$_3$-poor air transported from the Arctic had an appreciable influence on surface O$_3$ variability at THD for the samples analyzed. We note that the magnitude of [Acetylene]/[Benzene] is markedly lower for THD compared to the east coast studies. This is attributed to differences in source emission ratios (Warneke et al., 2007; Parrish et al., 2009) and transport patterns (Oltmans et al., 2008) impacting the Atlantic and Pacific Coasts.

3.4 Modeled sea ice exposure

FLEXPART was used to quantitatively determine the exposure of air masses intercepted by the R/V *Knorr* to first-year ice (FYI), multi-year ice (MYI), and total ICE (FYI+MYI). The term "exposure" used throughout this text is defined here as the modeled quantity (units of ppbv) of the specified type of inert FYI or MYI tracer, which is directly proportional to the time that an air mass was in contact with the specified types of sea ice. Examples of the modeling products used to determine the sea ice exposure for the air mass sampled on 2 April 2008 at 00:00 UTC are described here. Gas phase measurements from this period indicate that this air mass was exposed to halogen oxidation (refer to Fig. 2).
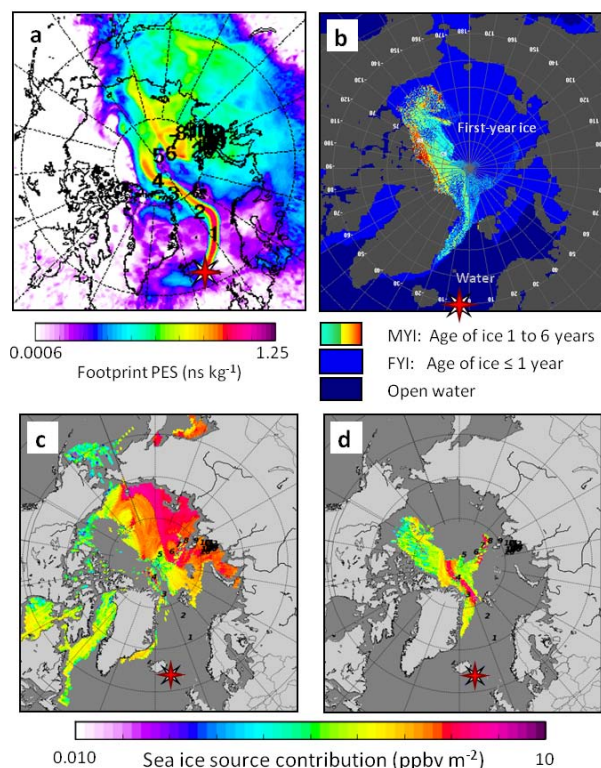

Fig. 4. (a) Circumpolar map of the FLEXPART modeled footprint potential emission sensitivity (PES) for the air mass sampled on 2 April 2008 at 00:00 UTC. The bold numbers represent the days of transport backward in time. **(b)** Map of the Arctic sea ice coverage colored by the modeled sea ice age for 1–7 April 2008. FLEXPART sea ice source contribution maps for **(c)** FYI and **(d)** MYI. The red star in panels (a–d) indicates the position of the R/V *Knorr* (62.9° N, 12.3° E).

A map of the FLEXPART footprint PES, shown in Fig. 4a, identifies where the released particles spent the most amount of time in the lowest 100 m of the atmosphere over their 20 day histories. The footprint PES map shows that this particular air mass remained largely intact for the first 5 days prior to arrival at the ship's location, but was broadly dispersed across the eastern Arctic further back in time. A map of the sea ice coverage colored by the modeled sea ice age for the week of 1–7 April 2008 is shown in Fig. 4b. The sea ice coverage was classified as FYI or MYI by the procedures outlined in Fowler et al. (2004).

The exposure of the sampled air mass to FYI or MYI was determined by folding the footprint PES with gridded sea ice coverage, which was assigned a unit emission flux of a FYI or MYI tracer. This results in the FYI and MYI source contribution maps shown in Fig. 4c and Fig. 4d, respectively, for the air intercepted on 2 April 2008 at 00:00 UTC. The sea ice source contribution maps (units of ppbv m^{-2}) depict the location and magnitude of the exposure of this particular air mass to FYI or MYI as quantified by the modeled abundance
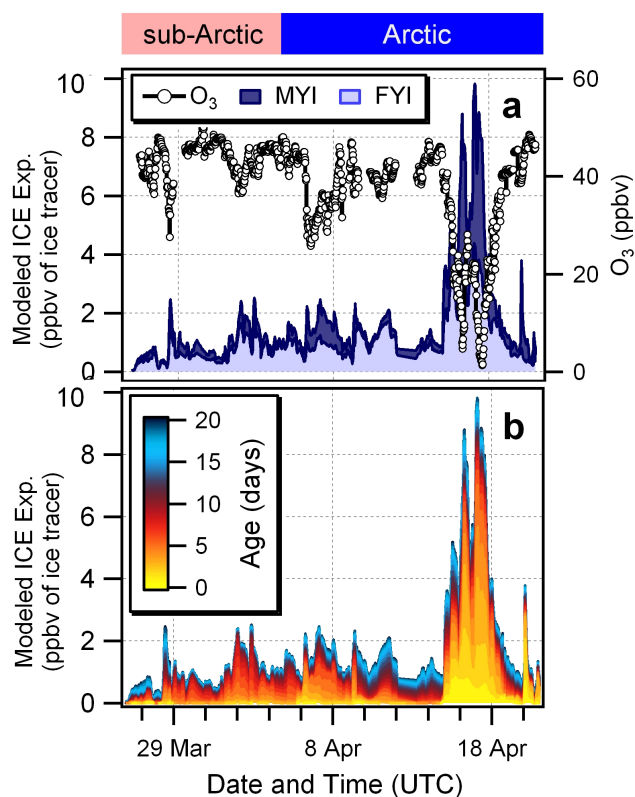
Fig. 5. (a) Time series of O_3 and the modeled FYI and MYI exposure for the sub-Arctic and Arctic data subsets from ICEALOT. MYI has been stacked on FYI so that the combined height represents the total ICE (FYI + MYI) exposure. **(b)** Time series of total ICE exposure colored by FLEXPART age.

of the FYI or MYI ice tracer (units of ppbv) over its 20 day history. The maps in Fig. 4 show that this air mass was transported over open water for approximately 3 days prior to sampling, exposed primarily to MYI in the western Arctic for the days 3–5 prior to sampling, and exposed mainly to FYI in the Siberian Arctic for days 5–20 of its modeled history.

The time series of the cumulative 20-day modeled exposure to FYI and MYI are shown in Fig. 5a. The two time series are stacked so that the cumulative value is equal to the total ICE exposure, which is shown in Fig. 5b. On average, exposure to FYI accounts for 68±15% and MYI accounts for 32±15% of the absolute exposure to total sea ice for the sub-Arctic and Arctic data subsets. This roughly scales with the relative surface areas of the two ice classes (Fig. 4b). As shown in Fig. 5a, O_3 exhibits a clear negative association with modeled ice exposure such that air masses with the greatest ICE exposure had the lowest measured O_3. Additionally, air masses with the largest depletions in O_3 (e.g., 6 April and 15–18 April 2008) have a larger than average contribution from MYI, which accounts for approximately 50-60% of the total ICE exposure for these events.

The time series of the total ICE exposure (Fig. 5b) is colored by the FLEXPART age, which is defined as the number of days backwards in time from the initial release of the particles. This figure shows that a wide range of FLEXPART ages contributed to the modeled ICE exposure. In the sub-Arctic region, air masses show larger contributions from the 5–15 day FLEXPART ages. This is in accordance with the greater time required for air masses exposed to sea ice covering the Arctic Ocean to be transported to latitudes as far south as 45° N. Consistently, the air masses with the largest contribution from 1-5 day FLEXPART ages were encountered in the Arctic when the ship was in close proximity (0.5 to 2.0 km) to sea ice.

The decrease in O_3 on 28 March 2008, previously described in Sect. 3.1 and highlighted in Fig. 2b, corresponds with a sharp increase in the modeled ICE exposure. FLEXPART source contribution maps show that this air mass was in contact with FYI in the Davis Strait and both Hudson and Baffin Bays as recently as 2–3 days prior to arrival at the R/V *Knorr*, while it required over 10 days of transport for the air mass to be exposed to MYI within the Arctic. This marks the most southerly latitude, 52° N, where an air mass with reduced O_3 due to halogen chemistry could be directly linked to significant exposure to sea ice by FLEXPART.

3.5 Correlations between O_3 and modeled sea ice exposure

Correlations between O_3 and the modeled exposure to FYI, MYI, and total ICE is used to determine if the variability in O_3 can be explained by the exposure to these types of sea ice. The depletion of O_3 is used here as a proxy for the presence of reactive halogens; however, the actual amount of O_3 destroyed is dependent on a number of variables including the initial concentration of O_3 within the air mass, the absolute concentrations of the halogens, the relative ratio between Br and Cl, and the reaction time in addition to several other factors.

If one type of ice were the dominant source of the reactive halogens responsible for the destruction of O_3 (i.e., a source region of reactive halogens), one would expect to see a stronger correlation between the exposure to that particular type of ice and the amount of O_3 destroyed assuming that all other reaction variables are similar.

The results of the linear correlations between the modeled exposures to FYI, MYI, and ICE versus O_3 are shown in Fig. 6. The linear correlation coefficients, r, are plotted as a function of FLEXPART age in Fig. 6a and Fig. 6b for the Arctic and combined Arctic and sub-Arctic data subsets, respectively. The FLEXPART ages are cumulative so that, for example, the modeled exposure on day 5 represents the sum of the exposure for days 1–5 of an air mass's history.

All of the correlations between the modeled sea ice exposures and O_3 are negative indicating that increased exposure to FYI, MYI, or ICE is directly associated with reduced
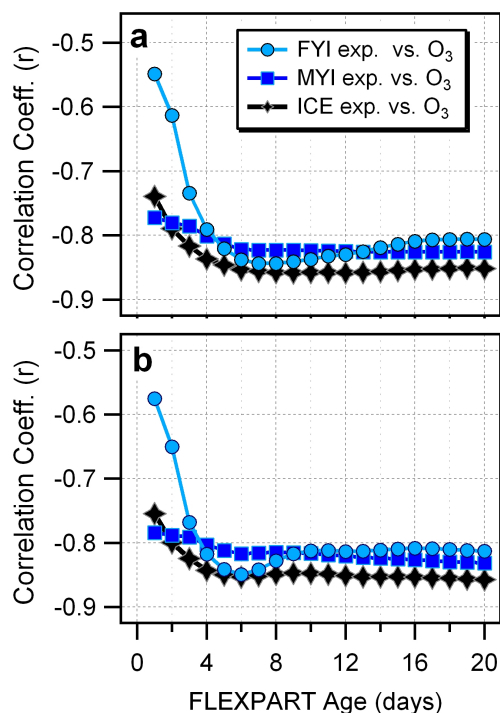
Fig. 6. Linear correlation coefficients for the modeled FYI, MYI, and ICE exposure versus O_3 as a function of the FLEXPART age for **(a)** the Arctic and **(b)** combined Arctic and sub-Arctic data subsets.

levels of O_3 in the Arctic and sub-Arctic marine boundary layer during the spring. O_3 correlated best with total ICE exposure for both data subsets. A mean correlation coefficient for ICE of $r = -0.86 \pm 0.03$ ($r^2 = 0.73$) suggests that up to 73% of the O_3 variability measured in the Arctic can be related to the modeled exposure to total ICE. As a sensitivity test, the correlation coefficients were also calculated for the same data subsets, but without the large-scale O_3 depletion. The correlation coefficient weakened from -0.86 to -0.60 indicating that this ODE was important but not solely responsible for the observed correlation between O_3 and the modeled ICE exposure.

There were very few air masses which had significant exposure to FYI within days 1–3 of its transport history resulting in poorer correlation coefficients for these FLEXPART ages. FYI appears to be slightly better correlated with O_3 than MYI for the 4–10 day ages, but the differences between exposure to FYI and MYI are small. This was partly due to the fact that the exposures to FYI and MYI were generally well correlated with one another ($0.70 < r < 0.87$) indicating that the air masses were sufficiently well dispersed so that they were often in contact with both types of ice at the same time. As a result of this co-linearity, the relative importance of exposure to FYI or MYI in determining O_3 variability remains inconclusive for the ICEALOT data set.
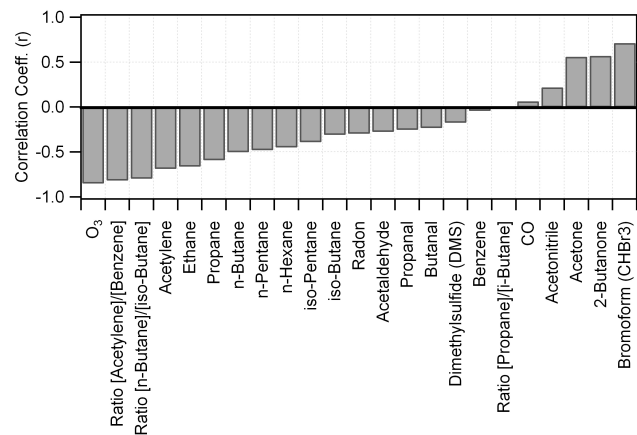
Fig. 7. Linear correlation coefficients for the 6-day cumulative modeled ICE exposure versus various gas-phase measurements made in the Arctic during ICEALOT.

The correlation coefficients for FYI, MYI and total ICE remain strong ($r < -0.80$) for all FLEXPART ages greater than 4 days. Here we examine the relative contribution of the total ICE exposure amassed in days 15–20 compared to the cumulative 20-day exposure in order to determine the fraction of air masses that remain over the sea ice in the Arctic footprint layer (i.e., lowest 100 m of the atmosphere) throughout their modeled histories. The median fractional contribution of the exposure amassed in days 15–20 compared to the cumulative 20 day air mass history is 0.18 for the Arctic data subset, indicating that 18% of the modeled exposure to total ICE occurred during the oldest 5 days of its 20-day history. This is not a negligible fraction of the cumulative exposure suggesting that the lifetimes of certain air masses within the Arctic boundary layer can be quite long. This is in general agreement with the results of Stohl (2006) who used FLEX-PART in a long-term global simulation of transport into the Arctic. It was determined in that study that the mean "arctic age," defined as the time the air resides continuously north of 70° N increased from 7 days in the winter to 14 days in the summer.

3.6 Correlations between other gases and modeled sea ice exposure

The modeled sea ice exposure is compared to other trace gases measured aboard the R/V *Knorr* in order to demonstrate the sensitivity of the model to the source region where halogen oxidation chemistry likely occurs. The linear correlation coefficients for the 6-day cumulative ICE exposure versus various gas-phase measurements made in the Arctic are compiled in Fig. 7. The 6-day ICE exposure was chosen because it represents the shortest amount of time to produce the strongest correlation with O_3 (Fig. 6a). O_3 and the halogen oxidation markers [Acetylene]/[Benzene] and [i-Butane]/[n-Butane] have the strongest negative correlations.

This is consistent with the variability of these species being heavily influenced by halogen oxidation. [Acetylene]/[Benzene] has a stronger correlation with ICE exposure than acetylene alone reiterating the facts that 1) destruction of acetylene by halogen oxidation drives the variability of [Acetylene]/[Benzene], and 2) the ratio is less sensitive to the influence of mixing and dilution than the absolute mixing ratio of acetylene alone.

The correlation coefficients for the C2-C6 alkanes are negative and generally increase with increasing carbon number. The oxidation of alkanes by Cl produces aldehydes and ketones, but the differences in the reactivities of these oxidized products with Cl and Br also influence their abundance. Aldehydes are highly reactive with both Cl and Br resulting in their reduction during ODEs on short timescales (Cavender et al., 2008). This is in accordance with the negative correlations of aldehydes with ICE exposure shown in Fig. 7. Ketones are produced from alkane + Cl reaction faster than they are destroyed by ketone + Cl reaction (Cavender et al., 2008). The net production of ketones from halogen oxidation results in the positive correlation. High concentrations of ketones have also been found in the snow-pack (Domine and Shepson, 2002; Grannas et al., 2002). Emissions of these compounds from the snow would further strengthen the positive correlation between ketones and ICE exposure.

Both radon and dimethyl sulfide (DMS) have weakly negative correlations with ICE exposure, which are qualitatively examined here. Atmospheric sources of radon are land-based whereas DMS is of oceanic origin (Ferek et al., 1995); therefore, the concentrations of these species are expected to be smaller in air masses that have been exposed to ICE rather than land or open water. Additionally, DMS can react with BrO (Barnes et al., 1991), which is an intermediate species that is present in elevated levels during ODEs (Hausmann and Platt, 1994; Neuman et al., 2010). Therefore, the oxidation of DMS by BrO would further enhance the negative correlation between DMS and ICE exposure.

Conversely, trace gases with atmospheric sinks other than ICE should exhibit positive correlations. The more time that an air parcel is exposed to sea ice, the lower the possibility of surface uptake by exposure to open water or land. This is true for acetonitrile, which has an oceanic sink (de Gouw et al., 2003; Jost et al., 2003). Benzene, CO, and [Propane]/[i-Butane], which is used here as an OH oxidation marker, have the weakest correlations with ICE exposure ($r < 0.05$). Compounds like benzene and CO have relatively long atmospheric lifetimes, are not sensitive to halogen oxidation, and do not have strong sources or sinks within the ice- and snow-covered Arctic.

Bromoform ($CHBr_3$) exhibits the strongest positive correlation with ICE exposure ($r = 0.71$). Like DMS, $CHBr_3$ has known oceanic sources (Cota and Sturges, 1997). If the presence of $CHBr_3$ is simply due to its oceanic source, it would be expected to have a negative correlation as does DMS even though the sources of DMS and $CHBr_3$ within the ocean can

be quite different. The strong positive correlation between $CHBr_3$ and the modeled ICE exposure suggests that sea ice is possibly a direct source of $CHBr_3$ and/or $CHBr_3$ may be produced during O_3 depletion chemistry.

4 Summary

The influence of halogen oxidation on the variability of O_3 and VOCs in the Arctic and sub-Arctic boundary layer was investigated using field measurements from multiple studies conducted in March and April 2008 as part of the PO-LARCAT project. Ship-based measurements conducted in the ice-free regions of the North Atlantic and Arctic Oceans significantly expanded upon the existing spatial and temporal database of VOCs in the Arctic and sub-Arctic springtime marine boundary layer. The wide geographic area sampled by the ship provided unique insights on the influence of halogen destruction of surface O_3 in the northern high latitudes and the transport of O_3-poor air masses from the Arctic Basin to latitudes as far south as 52° N.

The VOC ratios [Propane]/[i-Butane], [n-Butane]/[i-Butane], and [Acetylene]/[Benzene] were used as markers for of OH, Cl, and Br+Cl oxidation, respectively. The correlation between [Acetylene]/[Benzene] and O_3 was used to assess the influence of halogen oxidation on surface O_3 variability. This correlation strengthened as the R/V *Knorr* sailed northward towards the Arctic. O_3 was highly correlated with [Acetylene]/[Benzene] with $r = 0.98$ for the 544 data points collected north of 68° N suggesting that halogen oxidation accounted for up to 96% of the variability in O_3 measured in the springtime Arctic marine boundary layer during this study.

The strong correlation between [Acetylene]/[Benzene] and O_3 observed aboard the ship was substantiated by concurrent airborne and ground-based measurements within the Alaskan Arctic. This implies that halogen oxidation can account for the vast majority of the observed O_3 variability throughout the Arctic boundary layer during these springtime studies. The analysis was further expanded to include the sub-Arctic (45° N to 68° N) and two coastal mid-latitude sites (~40° N) in order to investigate the broader, spatial-scale variations in O_3. The results of this analysis indicated that halogen oxidation, which likely occurred in the Arctic high latitudes, influenced O_3 variability in the sub-Arctic; however, this influence did not extend to either of the coastal mid-latitude sites. The potential of this influence of Arctic air on more southerly latitudes warrants further investigation.

FLEXPART, a Lagrangian particle dispersion model, was used to quantitatively determine the exposure of air masses intercepted by the ship to first-year ice (FYI), multi-year ice (MYI), and ICE (FYI+MYI). The modeled sea ice exposures were negatively correlated with O_3 indicating that increased exposure to all types of Arctic sea ice was associated with reduced levels of O_3 in the Arctic and sub-Arctic marine

boundary layer during this springtime study. The modeled ICE exposure was compared to other gases measured aboard the R/V *Knorr*. Compounds that were negatively correlated with sea ice emissions were those that are readily oxidized by the reactive halogens Cl or Br or have atmospheric sources other than sea ice (e.g., ocean or land). Species that exhibited positive correlations were those that are produced from halogen oxidation or have atmospheric sinks other than sea-ice (e.g., ocean uptake or deposition). $CHBr_3$ had the strongest positive correlation with the modeled ICE exposure ($r = 0.71$), suggesting that arctic sea ice is possibly a direct source of $CHBr_3$ and/or $CHBr_3$ may be produced during O_3 depletion chemistry.

Edited by: J. W. Bottenheim

References

Atkinson, R. and Aschmann, S. A.: Kinetics of the gas phase reaction of Cl atoms with a series of organics at 296 +/- 2K and atmospheric pressure, Int. J. Chem. Kinet., 17, 33–41, 1985.

Atkinson, R.: Kinetics and mechanisms of the gas-phase reactions of the hydroxyl radical with organic-compounds under atmospheric conditions, Chem. Rev., 86, 69–201, 1986.

Atkinson, R., Baulch, D. L., Cox, R. A., Crowley, J. N., Hampson, J. R. F., Kerr, J. A., Rossi, M. J., and Troe, J.: Summary of evaluated kinetic and photochemical data for atmospheric chemistry, IUPAC Gas Kinetic Data Evalu. for Atmos. Chem., Web Version December 2001, 1–56, 2001.

Atkinson, R.: Kinetics of the gas-phase reactions of OH radicals with alkanes and cycloalkanes, Atmos. Chem. Phys., 3, 2233–2307, 2003,
http://www.atmos-chem-phys.net/3/2233/2003/.

Barnes, I., Bastian, V., Becker, K. H., and Overath, R. D.: Kinetic studies of the reactions of IO, BrO, and ClO with dimethylsulfide, Int. J. Chem. Kinet., 23, 579–591, 1991.

Barnes, I., Becker, K. H., and Overath, R. D.: Oxidation of organic sulfur compounds, in: Tropospheric Chemistry of Ozone in Polar Regions, edited by: Niki, H., and Becker, K. H., Springer-Verlag, New York, USA, 1993.

Barrie, L. and Platt, U.: Arctic tropospheric chemistry: an overview, Tellus B, 49, 450–454, 1997.

Barrie, L. A., Bottenheim, J. W., Schnell, R. C., Crutzen, P. J., and Rasmussen, R. A.: Ozone destruction and photochemical reactions at polar sunrise in the lower Arctic atmosphere, Nature, 334, 138–141, 1988.

Bates, T. S., Quinn, P. K., Coffman, D., Schulz, K., Covert, D. S., Johnson, J. E., Williams, E. J., Lerner, B. M., Angevine, W. M., Tucker, S. C., Brewer, W. A., and Stohl, A.: Boundary layer aerosol chemistry during TexAQS/GoMACCS 2006: Insights into aerosol sources and transformation processes, J. Geophys. Res.-Atmos., 113, D00F01, doi:10.1029/2008jd010023, 2008.

Belchansky, G. I., Douglas, D. C., and Platonov, N. G.: Spatial and temporal variations in the age structure of Arctic sea ice, Geophys. Res. Lett., 32, L18504, doi:10.1029/2005gl023976, 2005.

Bottenheim, J. W., Barrie, L. A., Atlas, E., Heidt, L. E., Niki, H., Rasmussen, R. A., and Shepson, P. B.: Depletion of lower tropospheric ozone during Arctic spring – The Polar Sunrise Experiment 1988, J. Geophys. Res.-Atmos., 95, 18555–18568, 1990.

Bottenheim, J. W., Netcheva, S., Morin, S., and Nghiem, S. V.: Ozone in the boundary layer air over the Arctic Ocean: measurements during the TARA transpolar drift 2006–2008, Atmos. Chem. Phys., 9, 4545–4557, doi:10.5194/acp-9-4545-2009, 2009.

Cavender, A. E., Biesenthal, T. A., Bottenheim, J. W., and Shepson, P. B.: Volatile organic compound ratios as probes of halogen atom chemistry in the Arctic, Atmos. Chem. Phys., 8, 1737–1750, doi:10.5194/acp-8-1737-2008, 2008.

Cota, G. F. and Sturges, W. T.: Biogenic bromine production in the Arctic, Mar. Chem., 56, 181–192, 1997.

Cuevas, C. A., Notario, A., Martinez, E., and Albaladejo, J.: Temperature-dependence study of the gas-phase reactions of atmospheric Cl atoms with a series of aliphatic aldehydes, Atmos. Environ., 40, 3845–3854, doi:10.1016/j.atmosenv.2006.03.001, 2006.

de Gouw, J. A., Goldan, P. D., Warneke, C., Kuster, W. C., Roberts, J. M., Marchewka, M., Bertman, S. B., Pszenny, A. A. P., and Keene, W. C.: Validation of proton transfer reaction-mass spectrometry (PTR-MS) measurements of gas-phase organic compounds in the atmosphere during the New England Air Quality Study (NEAQS) in 2002, J. Geophys. Res.-Atmos., 108, D214682, doi:10.1029/2003jd003863, 2003.

DeMore, W. B., Sander, S. P., Golden, D. M., Hampson, R. F., Kurylo, M. J., Howard, C. J., Ravishankara, A. R., Kolb, C. E., and Molina, M. J.: Chemical kinetics and photochemical data for use in stratospheric modeling. Evaluation number 12, JPL Pub., 1–266, 1997.

Domine, F. and Shepson, P. B.: Air-snow interactions and atmospheric chemistry, Science, 297, 1506–1510, 2002.

Ferek, R. J., Hobbs, P. V., Radke, L. F., Herring, J. A., Sturges, W. T., and Cota, G. F.: Dimethyl sulfide in the arctic atmosphere, J. Geophys. Res.-Atmos., 100, 26093–26104, 1995.

Fowler, C., Emery, W. J., and Maslanik, J.: Satellite-derived evolution of Arctic sea ice age: October 1978 to March 2003, IEEE Geosci. Remote S., 1, 71-74, doi:10.1109/lgrs.2004.824741, 2004.

Gerbig, C., Schmitgen, S., Kley, D., Volz-Thomas, A., Dewey, K., and Haaks, D.: An improved fast-response vacuum-UV resonance fluorescence CO instrument, J. Geophys. Res.-Atmos., 104, 1699–1704, 1999.

Goldan, P. D., Kuster, W. C., Williams, E., Murphy, P. C., Fehsenfeld, F. C., and Meagher, J.: Nonmethane hydrocarbon and oxy hydrocarbon measurements during the 2002 New England

Air Quality Study, J. Geophys. Res.-Atmos., 109, D21309, doi:10.1029/2003JD004455, 2004.

Grannas, A. M., Shepson, P. B., Guimbaud, C., Sumner, A. L., Albert, M., Simpson, W., Domine, F., Boudries, H., Bottenheim, J., Beine, H. J., Honrath, R., and Zhou, X. L.: A study of photochemical and physical processes affecting carbonyl compounds in the Arctic atmospheric boundary layer, Atmos. Environ., 36, 2733–2742, 2002.

Hausmann, M., and Platt, U.: Spectroscopic measurement of bromine oxide and ozone in the high Arctic during Polar Sunrise Experiment 1992, J. Geophys. Res.-Atmos., 99, 25399–25413, 1994.

Hirdman, D., Sodemann, H., Eckhardt, S., Burkhart, J. F., Jefferson, A., Mefford, T., Quinn, P. K., Sharma, S., Strom, J., and Stohl, A.: Source identification of short-lived air pollutants in the Arctic using statistical analysis of measurement data and particle dispersion model output, Atmos. Chem. Phys., 10, 669–693, doi:10.5194/acp-10-669-2010, 2010.

Hopper, J. F., Barrie, L. A., Silis, A., Hart, W., Gallant, A. J., and Dryfhout, H.: Ozone and meteorology during the 1994 Polar Sunrise Experiment, J. Geophys. Res.-Atmos., 103, 1481–1492, 1998.

Jobson, B. T., Niki, H., Yokouchi, Y., Bottenheim, J., Hopper, F., and Leaitch, R.: Measurements of C2-C6 hydrocarbons during the Ploar Sunrise 1992 Experiment – Evidence for Cl and Br atom chemistry, J. Geophys. Res.-Atmos., 99, 25355-25368, 1994.

Jost, C., Trentmann, J., Sprung, D., Andreae, M. O., and Dewey, K.: Deposition of acetonitrile to the Atlantic Ocean off Namibia and Angola and its implications for the atmospheric budget of acetonitrile, Geophys. Res. Lett., 30, 1837, doi:10.1029/2003gl017347, 2003.

Kaleschke, L., Richter, A., Burrows, J., Afe, O., Heygster, G., Notholt, J., Rankin, A. M., Roscoe, H. K., Hollwedel, J., Wagner, T., and Jacobi, H. W.: Frost flowers on sea ice as a source of sea salt and their influence on tropospheric halogen chemistry, Geophys. Res. Lett., 31, L16114, doi:10.1029/2004gl020655, 2004.

Kamboures, M. A., Hansen, J. C., and Francisco, J. S.: A study of the kinetics and mechanisms involved in the atmospheric degradation of bromoform by atomic chlorine, Chem. Phys. Lett., 353, 335–344, 2002.

Keene, W. C., Stutz, J., Pszenny, A. A. P., Maben, J. R., Fischer, E. V., Smith, A. M., von Glasow, R., Pechtl, S., Sive, B. C., and Varner, R. K.: Inorganic chlorine and bromine in coastal New England air during summer, J. Geophys. Res.-Atmos., 112, D10S12, doi:10.1029/2006jd007689, 2007.

Lerner, B. M., Gilman, J. B., Murphy, P. C., Kuster, W. C., Burkhart, J. F., Stohl, A., Hermansen, O., Wolfe, D., Hazen, D., de Gouw, J. A., and Williams, E. J.: Observation and characterization of ozone depletion events in the Arctic Ocean during ICEALOT, in preparation, 2010.

Martin, S., Drucker, R., and Fort, M.: A laboratory study of frost flower growth on the surface of young sea ice, J. Geophys. Res.-Oceans, 100, 7027–7036, 1995.

McConnell, J. C., Henderson, G. S., Barrie, L., Bottenheim, J., Niki, H., Langford, C. H., and Templeton, E. M. J.: Photochemical bromine production implicated in Arctic boundary layer ozone depletion, Nature, 355, 150–152, 1992.

Montzka, S. A., Myers, R. C., Butler, J. H., Elkins, J. W., and Cummings, S. O.: Global tropospheric distribution and calibration scale of HCFC-22, Geophys. Res. Lett., 20, 703–706, 1993.

Neuman, J. A., Nowak, J. B., Huey, L. G., Burkholder, J. B., Dibb, J. E., Holloway, J. S., Liao, J., Peischl, J., Roberts, J. M., Ryerson, T. B., Scheuer, E., Stark, H., Stickel, R. E., Tanner, D. J., and Weinheimer, A.: Bromine measurements in ozone depleted air over the Arctic Ocean, Atmos. Chem. Phys., 10, 6503–6514, 10, http://www.atmos-chem-phys.net/10/6503/10/.5194/acp-10-6503-2010, 2010.

Notz, D. and Worster, M. G.: In situ measurements of the evolution of young sea ice, J. Geophys. Res.-Oceans, 113, C03001, doi:10.1029/2007jc004333, 2008.

Oltmans, S. J. and Komhyr, W. D.: Surface ozone distributions and variations from 1973–1984 Measurements at the NOAA Geophysical Monitoring for Climatic-Change Base-line Observatories, J. Geophys. Res.-Atmos., 91, 5229–5236, 1986.

Oltmans, S. J., Schnell, R. C., Sheridan, P. J., Peterson, R. E., Li, S. M., Winchester, J. W., Tans, P. P., Sturges, W. T., Kahl, J. D., and Barrie, L. A.: Seasonal surface ozone and filterable bromine relationship in the high Arctic, Atmos. Environ., 23, 2431–2441, 1989.

Oltmans, S. J. and Levy, H.: Surface ozone measurements from a global network, Atmos. Environ., 28, 9–24, 1994.

Oltmans, S. J., Lefohn, A. S., Harris, J. M., and Shadwick, D. S.: Background ozone levels of air entering the west coast of the US and assessment of longer-term changes, Atmos. Environ., 42, 6020–6038, doi:10.1016/j.atmosenv.2008.03.034, 2008.

Parrish, D. D., Stohl, A., Forster, C., Atlas, E. L., Blake, D. R., Goldan, P. D., Kuster, W. C., and de Gouw, J. A.: Effects of mixing on evolution of hydrocarbon ratios in the troposphere, J. Geophys. Res.-Atmos., D10S34, doi:10.1029/2006jd007583, 2007.

Parrish, D. D., Kuster, W. C., Shao, M., Yokouchi, Y., Kondo, Y., Goldan, P. D., de Gouw, J. A., Koike, M., and Shirai, T.: Comparison of air pollutant emissions among mega-cities, Atmos. Environ., 43, 6435–6441, doi:10.1016/j.atmosenv.2009.06.024, 2009.

Ramacher, B., Rudolph, J., and Koppmann, R.: Hydrocarbon measurements during tropospheric ozone depletion events: Evidence for halogen atom chemistry, J. Geophys. Res.-Atmos., 104, 3633–3653, 1999.

Ramacher, B., Orlando, J. J., and Tyndall, G. S.: Temperature-dependent rate coefficient measurements for the reaction of bromine atoms with a series of aldehydes, Int. J. Chem. Kinet., 32, 460–465, 2000.

Ridley, B. A., Atlas, E. L., Montzka, D. D., Browell, E. V., Cantrell, C. A., Blake, D. R., Blake, N. J., Cinquini, L., Coffey, M. T., Emmons, L. K., Cohen, R. C., DeYoung, R. J., Dibb, J. E., Eisele, F. L., Flocke, F. M., Fried, A., Grahek, F. E., Grant, W. B., Hair, J. W., Hannigan, J. W., Heikes, B. J., Lefer, B. L., Mauldin, R. L., Moody, J. L., Shetter, R. E., Snow, J. A., Talbot, R. W., Thornton, J. A., Walega, J. G., Weinheimer, A. J., Wert, B. P., and Wimmers, A. J.: Ozone depletion events observed in the high latitude surface layer during the TOPSE aircraft program, J. Geophys. Res.-Atmos., 108, 8356, doi:10.1029/2001jd001507, 2003.

Ryerson, T. B., Buhr, M. P., Frost, G. J., Goldan, P. D., Holloway, J. S., Hubler, G., Jobson, B. T., Kuster, W. C., McKeen, S. A., Parrish, D. D., Roberts, J. M., Sueper, D. T., Trainer, M., Williams, J., and Fehsenfeld, F. C.: Emissions lifetimes and ozone for-

mation in power plant plumes, J. Geophys. Res.-Atmos., 103, 22569–22583, 1998.

Seibert, P. and Frank, A.: Source-receptor matrix calculation with a Lagrangian particle dispersion model in backward mode, Atmos. Chem. Phys., 4, 51–63, doi:10.5194/acp-4-51-2004, 2004.

Simpson, W. R., Carlson, D., Honninger, G., Douglas, T. A., Sturm, M., Perovich, D., and Platt, U.: First-year sea-ice contact predicts bromine monoxide (BrO) levels at Barrow, Alaska better than potential frost flower contact, Atmos. Chem. Phys., 7, 621–627, doi:10.5194/acp-7-621-2007, 2007a.

Simpson, W. R., von Glasow, R., Riedel, K., Anderson, P., Ariya, P., Bottenheim, J., Burrows, J., Carpenter, L. J., Friess, U., Goodsite, M. E., Heard, D., Hutterli, M., Jacobi, H. W., Kaleschke, L., Neff, B., Plane, J., Platt, U., Richter, A., Roscoe, H., Sander, R., Shepson, P., Sodeau, J., Steffen, A., Wagner, T., and Wolff, E.: Halogens and their role in polar boundary-layer ozone depletion, Atmos. Chem. Phys., 7, 4375–4418, doi:10.5194/acp-7-4375-2007, 2007b.

Solberg, S., Schmidbauer, N., Semb, A., Stordal, F., and Hov, O.: Boundary-layer ozone depletion as seen in the Norwegian Arctic in Spring, J. Atmos. Chem., 23, 301–332, 1996.

Stohl, A., Hittenberger, M., and Wotawa, G.: Validation of the Lagrangian particle dispersion model FLEXPART against large-scale tracer experiment data, Atmos. Environ., 32, 4245–4264, 1998.

Stohl, A., Eckhardt, S., Forster, C., James, P., Spichtinger, N., and Seibert, P.: A replacement for simple back trajectory calculations in the interpretation of atmospheric trace substance measurements, Atmos. Environ., 36, 4635–4648, 2002.

Stohl, A., Forster, C., Eckhardt, S., Spichtinger, N., Huntrieser, H., Heland, J., Schlager, H., Wilhelm, S., Arnold, F., and Cooper, O.: A backward modeling study of intercontinental pollution transport using aircraft measurements, J. Geophys. Res.-Atmos., 108, 4370, doi:10.1029/2002jd002862, 2003.

Stohl, A., Forster, C., Frank, A., Seibert, P., and Wotawa, G.: Technical note: The Lagrangian particle dispersion model FLEXPART version 6.2, Atmos. Chem. Phys., 5, 2461–2474, doi:10.5194/acp-5-2461-2005, 2005.

Stohl, A.: Characteristics of atmospheric transport into the Arctic troposphere, J. Geophys. Res.-Atmos., 111, D11306, doi:10.1029/2005jd006888, 2006.

Sturges, W. T., Schnell, R. C., Landsberger, S., Oltmans, S. J., Harris, J. M., and Li, S. M.: Chemical and meterological influences on surface ozone destruction at Barrow, Alaska, during Spring 1989, Atmos. Environ., 27, 2851–2863, 1993.

Wagner, T., Leue, C., Wenig, M., Pfeilsticker, K., and Platt, U.: Spatial and temporal distribution of enhanced boundary layer BrO concentrations measured by the GOME instrument aboard ERS-2, J. Geophys. Res.-Atmos., 106, 24225–24235, 2001.

Wallington, T. J., and Kurylo, M. J.: The gas-phase reactions of hydroxyl radicals with a series of aliphatic alcohols over the temperature range 240-440 K, Int. J. Chem. Kinet., 19, 1015–1023, 1987.

Wallington, T. J., Skewes, L. M., and Siegl, W. O.: Kinetics of the gas-phase reaction of chlorine atoms with a series of alkenes, alkynes and aromatic species at 298 K, J Photoch. Photobio. A, 45, 167–175, 1988.

Wallington, T. J., Skewes, L. M., Siegl, W. O., and Japar, S. M.: A relative rate study of the reaction of bromine atoms with a variety of organic compounds at 298 K, Int. J. Chem. Kinet., 21, 1069–1076, 1989.

Warneke, C., McKeen, S. A., de Gouw, J. A., Goldan, P. D., Kuster, W. C., Holloway, J. S., Williams, E. J., Lerner, B. M., Parrish, D. D., Trainer, M., Fehsenfeld, F. C., Kato, S., Atlas, E. L., Baker, A., and Blake, D. R.: Determination of urban volatile organic compound emission ratios and comparison with an emissions database, J. Geophys. Res.-Atmos., 112, D10S47, doi:10.1029/2006jd007930, 2007.

Warneke, C., Bahreini, R., Brioude, J., Brock, C. A., de Gouw, J. A., Fahey, D. W., Froyd, K. D., Holloway, J. S., Middlebrook, A., Miller, L., Montzka, S., Murphy, D. M., Peischl, J., Ryerson, T. B., Schwarz, J. P., Spackman, J. R., and Veres, P.: Biomass burning in Siberia and Kazakhstan as an important source for haze over the Alaskan Arctic in April 2008, Geophys. Res. Lett., 36, L02813, doi:10.1029/2008gl036194, 2009.

Warneke, C., Froyd, K. D., Brioude, J., Bahreini, R., Brock, C. A., Cozic, J., de Gouw, J. A., Fahey, D. W., Ferrare, R., Holloway, J. S., Middlebrook, A. M., Miller, L., Montzka, S., Schwarz, J. P., Sodemann, H., Spackman, J. R., and Stohl, A.: An important contribution to springtime Arctic aerosol from biomass burning in Russia, Geophys. Res. Lett., 37, L01801, doi:10.1029/2009gl041816, 2010.

Zhao, Z., Huskey, D. T., Nicovich, J. M., and Wine, P. H.: Temperature-dependent kinetics study of the gas-phase reactions of atomic chlorine with acetone, 2-butanone, and 3-pentanone, Int. J. Chem. Kinet., 40, 259–267, doi:10.1002/kin.20321, 2008.